E-Article

The Geography of Morphological Convergence in the Radiations of Pacific *Sebastes* Rockfishes

Travis Ingram[1,*] **and Yoshiaki Kai**[2]

1. Department of Zoology, University of Otago, Dunedin 9054, New Zealand; 2. Maizuru Fisheries Research Station, Field Science Education and Research Center, Kyoto University, Nagahama, Maizuru, Kyoto 625-0086, Japan

Submitted August 15, 2013; Accepted May 8, 2014; Electronically published October 6, 2014

Online enhancement: appendix. *Dryad data:* http://dx.doi.org/10.5061/dryad.s5s3s.

abstract: The evolution of convergent phenotypes in lineages subject to similar selective pressures is a common feature of adaptive radiation. In geographically replicated radiations, repeated convergence occurs between clades occupying distinct regions or islands. Alternatively, a clade may repeatedly reach the same adaptive peaks in broadscale sympatry, resulting in extensive convergence within a region. Rockfish (*Sebastes* sp.) have radiated in both the northeast and northwest Pacific, allowing tests of the extent and geographic pattern of convergence in a marine environment. We used a suite of phylogenetically informed methods to test for morphological convergence in rockfish. We examined patterns of faunal similarity using nearest neighbor distances in morphospace and the frequency of morphologically similar yet distantly related species pairs. The extent of convergence both between regions and within the northeast Pacific exceeds the expectation under a Brownian motion null model, although constraints on trait space could account for the similarity. We then used a recently developed method (SURFACE) to identify adaptive peak shifts in *Sebastes* evolutionary history. We found that the majority of convergent peak shifts occur within the northeast Pacific rather than between regions and that the signal of peak shifts is strongest for traits related to trophic morphology. Pacific rockfish thus demonstrate a tendency toward morphological convergence within one of the two broad geographic regions in which they have diversified.

Keywords: adaptive radiation, clade-wide convergence, Hansen model, Ornstein-Uhlenbeck model, replicated radiation, SURFACE.

Introduction

The convergent evolution of similar phenotypes in response to shared ecological conditions provides powerful evidence for natural selection and is a hallmark of many adaptive radiations (Schluter 2000; Losos 2010). In extreme cases, replicated adaptive radiation occurs when clades diversifying independently in multiple regions produce similar sets of convergent species, implying that the radiations have a strong deterministic component (Schluter 1990, 2000). The study of replicated radiation has focused on islands and island-like habitats such as young lakes, where similar environments and a wealth of available resources relative to the number of competing species can set the stage for colonizing lineages to diversify into the same niches on each island (Kocher et al. 1993; Losos et al. 1998; Chiba 2004; Gillespie 2004; Mahler et al. 2013). Convergence between lineages occupying larger regions such as continents or oceans, including classic examples of matched pairs of marsupial and eutherian mammals (Springer et al. 2004), is well established, but replicated radiation across entire clades has rarely been tested or demonstrated in continental or marine faunas. Instead, an alternative outcome—convergence of multiple lineages within a shared region—has recently been demonstrated in continental (Kozak et al. 2009), marine (Rutschmann et al. 2011; Frédérich et al. 2013), and large lacustrine (Muschick et al. 2012) radiations, with phenotypically similar lineages often occurring in broad sympatry. These outcomes—clade-wide convergence between or within regions—present alternative geographic contexts in which convergence can take place.

Advances in comparative methods and increased availability of molecular phylogenetic trees are making possible targeted tests for convergence in clades undergoing adaptive radiation. Historically, phylogenetic approaches have compared the statistical pattern of faunal similarity to null distributions, initially obtained by randomization and later by simulation under evolutionary null models such as Brownian motion (e.g., Cody and Mooney 1978; Ricklefs and Travis 1980; Muschick et al. 2012). These methods do not incorporate processes that can result in deterministic convergence, such as adaptation toward the same optimum trait values, often represented as multivariate peaks on a macroevolutionary adaptive landscape (Simpson 1953; Hansen 2012). Comparative methods based on the Ornstein-Uhlenbeck model have been used to represent evolutionary dynamics that include a stochastic compo-

* Corresponding author; e-mail: travis.ingram@otago.ac.nz.

Am. Nat. 2014. Vol. 184, pp. E115–E131.
DOI: 10.1086/678053

nent and deterministic adaptation toward one or more peaks (Hansen 1997; Butler and King 2004; Beaulieu et al. 2012). Most such approaches require an a priori hypothesis about which lineages are convergent, but extensions of this method allow convergent peak shifts to be identified using only a tree and data for multiple phenotypic traits (Ingram and Mahler 2013; Mahler et al. 2013). The resulting model includes estimates of the positions of the multivariate trait optima and can thus be regarded as an approximation of a macroevolutionary adaptive landscape. The inferred positions of peak shifts on the tree can be combined with reconstructed biogeographic histories of the clade to infer the geographic context of convergence (Mahler and Ingram 2014) and to test for clade-wide convergence either between geographically replicated radiations or within regions.

Rockfish of the genus *Sebastes* living in the North Pacific Ocean are an excellent system in which to test for clade-wide convergence between and within regions in a marine environment. With approximately 110 species worldwide, including 96 described species in the northern Pacific Ocean, this diverse genus is a dominant component of the northern temperate ichthyofauna (Nakabo and Kai 2013). At least 62 species occur exclusively in the northeast Pacific (NEP), while 28 are restricted to the northwest Pacific (NWP), and 5 have a trans-Pacific (TP) distribution. Dispersal out of the North Pacific has resulted in small numbers of species endemic to the Gulf of California (treated here as distinct from the NEP), the Atlantic Ocean, and the Southern Hemisphere. Since their Miocene origin (Hyde and Vetter 2007), rockfish have undergone rapid lineage diversification, accompanied by extensive diversification in resource use, habitat, and ecologically relevant morphology. Species vary in adult depth habitat (shallow subtidal to >500 m), in the use of benthic habitats versus the water column, and in the extent of feeding on zooplankton, larger invertebrates, or fishes (reflected in trophic position inferred using stable nitrogen isotope ratios). This ecological variation is accompanied by variation in body size (17–108 cm maximum total length), trophic morphology such as gill raker number and length, and elements of body and fin shapes (Love et al. 2002; Ingram and Shurin 2009; Ingram 2011).

While a quantitative appraisal of the extent of morphological convergence in *Sebastes* has yet to be carried out, the taxonomic history of the genus suggests that convergence may be common. Several previously recognized groupings within rockfish (variably designated genera or subgenera), identified on the basis of external morphology, contained species from both the NEP and the NWP (Matsubara 1943; Chen 1985; Kendall Jr. 2000), implying frequent dispersal between regions. However, later molecular studies clearly demonstrated that most of these groups were polyphyletic, consisting of NEP and NWP species that were distantly related despite their phenotypic resemblance (Kai et al. 2003; Hyde and Vetter 2007), and that dispersal between regions was relatively rare. Each region is home to substantial clades that have diversified in situ, and the NEP in particular contains multiple lineages that have independently arrived at similar ecological strategies (such as benthic vs. open-water habitat use; Love et al. 2002). This makes clade-wide convergence both between and within oceanic regions plausible outcomes in the radiations of *Sebastes* in the North Pacific.

Here, we use molecular phylogenies, measurements of morphological traits with putative links to ecology, and statistical and model-based comparative analyses to ask to what extent convergence has occurred between and within regions in Pacific *Sebastes*. We show that while some convergence between regions is evident, most cases of convergence occur between lineages within the northeast Pacific.

Methods

Phylogeny Reconstruction

The most complete phylogenetic treatment of *Sebastes* to date was presented by Hyde and Vetter (2007), who sequenced seven mitochondrial (cytochrome *b* [cyt *b*], cytochrome oxidase 1 [cox1], 12S rRNA, 16S rRNA, tRNA proline, tRNA threonine, and the control region) and two nuclear (RAG2 and ITS1) genes from 99 *Sebastes* species and four outgroup taxa. To this alignment, we added nine additional species from the NWP, four of which are members of species complexes that were only recently resolved as valid species (*Sebastes cheni*, *Sebastes ventricosus*, *Sebastes nudus*, and *Sebastes zonatus*; Kai and Nakabo 2008, 2013; Muto et al. 2011) and five of which had not been included in previous treatments (*Sebastes koreanus*, *Sebastes nivosus*, *Sebastes longispinis*, *Sebastes itinus*, and *Sebastes wakiyai*). We used existing mitochondrial DNA sequences for most of these additional species (Kai and Nakabo 2008, 2013; Muto et al. 2011) and added new sequences for *S. itinus* (gene, GenBank accession no.: cyt *b*, AB826452; cox1, AB826455; 12S rRNA, AB826456; 16S rRNA, AB826453; tRNAs and the control region, AB826454). Tissue suitable for DNA extraction was not available for *S. wakiyai*, so we incorporated this species in the tree using a topological constraint (see below). Sequences were manually aligned to Hyde and Vetter's (2007) alignment, with unrepresented genes coded as missing data. Thus, we were able to include all currently described species in the northern Pacific, with the exception of *Sebastes varispinis* in the NEP, which lacks sequence data and is known from only juvenile specimens.

We inferred time-calibrated phylogenetic trees of *Se-*

bastes and its relatives using Markov chain Monte Carlo (MCMC) analysis with the program BEAST (Drummond et al. 2012). We set priors on three calibration points to date the phylogeny. We set a strong normal prior (mean = 3, SD = 0.05) on the time of the most recent common ancestor of *Sebastes alutus* in the North Pacific and *Sebastes norvegicus* in the North Atlantic, based on the opening of the Bering Strait ca. 3 Ma (Hyde and Vetter 2007). We set a weak exponential prior (mean = 8) with a minimum age (offset) of 8 Myr on the most recent common ancestor of all extant *Sebastes*, consistent both with the age of fossil *Sebastes* from the upper Miocene (Jordan and Gilbert 1920) and with previous estimates of the crown age of *Sebastes* (Hyde and Vetter 2007). Finally, we set a weak normal prior on the root age (mean = 30, SD = 6.5) based on the distribution of divergence time estimates (95% credible interval [CI] 17–43 Myr) between *Sebastes* and the most distantly related outgroup, *Sebastolobus alascanus*, from a much broader phylogenetic study of actinopterygian fishes with 36 fossil calibrations (Near et al. 2012). We note that age estimates are expected to be dominated by the strong prior on the *S. alutus*–*S. norvegicus* divergence. To include *S. wakiyai* in the tree despite its lack of sequence data, we constrained it to be sister to *Sebastes steindachneri*, which is believed to be its closest relative (Barsukov 1981). As we have no information about the divergence date between these species, branching times were sampled from the tree prior, and the uncertainty in this branching time was thus incorporated into the posterior distribution of trees. As a starting tree, we used the maximum clade credibility (MCC) tree from a previous analysis (Ingram 2011) of Hyde and Vetter's (2007) alignment, ensuring that constraints were satisfied, and inserted the additional species into the tree near their suspected or known relatives.

Sequences were partitioned by gene, with the two tRNA genes grouped into one partition. We used PartitionFinder (Lanfear et al. 2012) to assess support for partitioning each protein coding gene into codons 1+2 and codon 3 (this was supported for each of cyt *b*, cox1, and RAG2) and to identify the best substitution model for each partition using the Bayesian information criterion (BIC). Favored models varied by partition, including GTR (cyt *b* codon 3, RAG2 codon 3), HKY (control region), K80 (16S rRNA), and TN93 with estimated (cyt *b* codons 1+2, ITS1, cox1 codon 3) or equal (tRNA pro + tRNA thr, RAG2 codons 1+2, cox1 codons 1+2) base frequencies. Mitochondrial gene 12S rRNA was best fit by a GTR model with equal base frequencies, but we found that the parameters of this model could not be sampled effectively even over 30 million generations, so we substituted the next best model (K80, ΔBIC = 1.1). Gamma-distributed rate heterogeneity (which we implemented with four rate categories) was supported for all partitions; a proportion of invariant sites was supported for all but cox1 codon 3.

We ran eight MCMC analyses of 30 million generations each, sampling every 2,500 generations. We used the program Tracer to assess convergence, determining that all evolutionary parameters and likelihoods had converged between runs and that sampling was well mixed (effective sample size of at least 200 for all parameters of interest). We conservatively discarded the first one-sixth of each run as burn-in, leaving 10,000 samples per run. We then thinned each tree sample by a factor of 40 before combining trees from the eight runs for a combined sample of 1,000 trees from the posterior distribution. We used the TreeAnnotator utility to identify the maximum clade credibility tree—the tree from this sample with the maximum summed posterior probabilities of nodes—and to compute branch lengths from the mean node heights across sampled trees (fig. A1; figs. A1–A5 available online). We also took every tenth tree from this sample to obtain a subsample of 100 trees, which we used in our morphological analyses to account for phylogenetic uncertainty.

For all subsequent analyses, we pruned the four outgroup taxa and 10 *Sebastes* species from regions other than the NEP or the NWP: four endemic to the Gulf of California (and isolated from the main NEP fauna), four in the Atlantic (*S. norvegicus* and three close relatives), and two in the Southern Hemisphere. We also removed two cryptic NEP species that had not been described at the time morphological data collection began: *Sebastes miniatus* "Type 2" (later named *Sebastes crocotulus*; Hyde et al. 2008) and *Sebastes saxicola* "N." Our categorization of species as NEP, NWP, or TP followed Love et al. (2002), modified to account for the subsequent recognition that *Sebastes aleutianus* and *Sebastes ciliatus* are restricted to the NEP, while their recently distinguished sister species (*Sebastes melanostictus* and *Sebastes variabilis*, respectively) have TP distributions (Orr and Blackburn 2004; Orr and Hawkins 2008). The three additional TP species that have at least part of their range in both the NEP and NWP are *S. alutus*, *Sebastes borealis*, and *Sebastes glaucus* (Love et al. 2002). Our pruned tree thus included 95 species: 62 NEP, 28 NWP, and 5 TP (fig. 1). The alignment file, the full MCC tree, and the pruned MCC tree have been deposited in TreeBase (study accession no. S15834).

Morphospace Construction

We measured 683 individual rockfish, primarily museum specimens but also including carcasses and whole fish obtained from research and commercial fishing vessels. These samples represented 94 species, with 1–45 individuals measured per species (mean 7.2) and most species (>80%) represented by 4–10 individuals. T. Ingram measured all

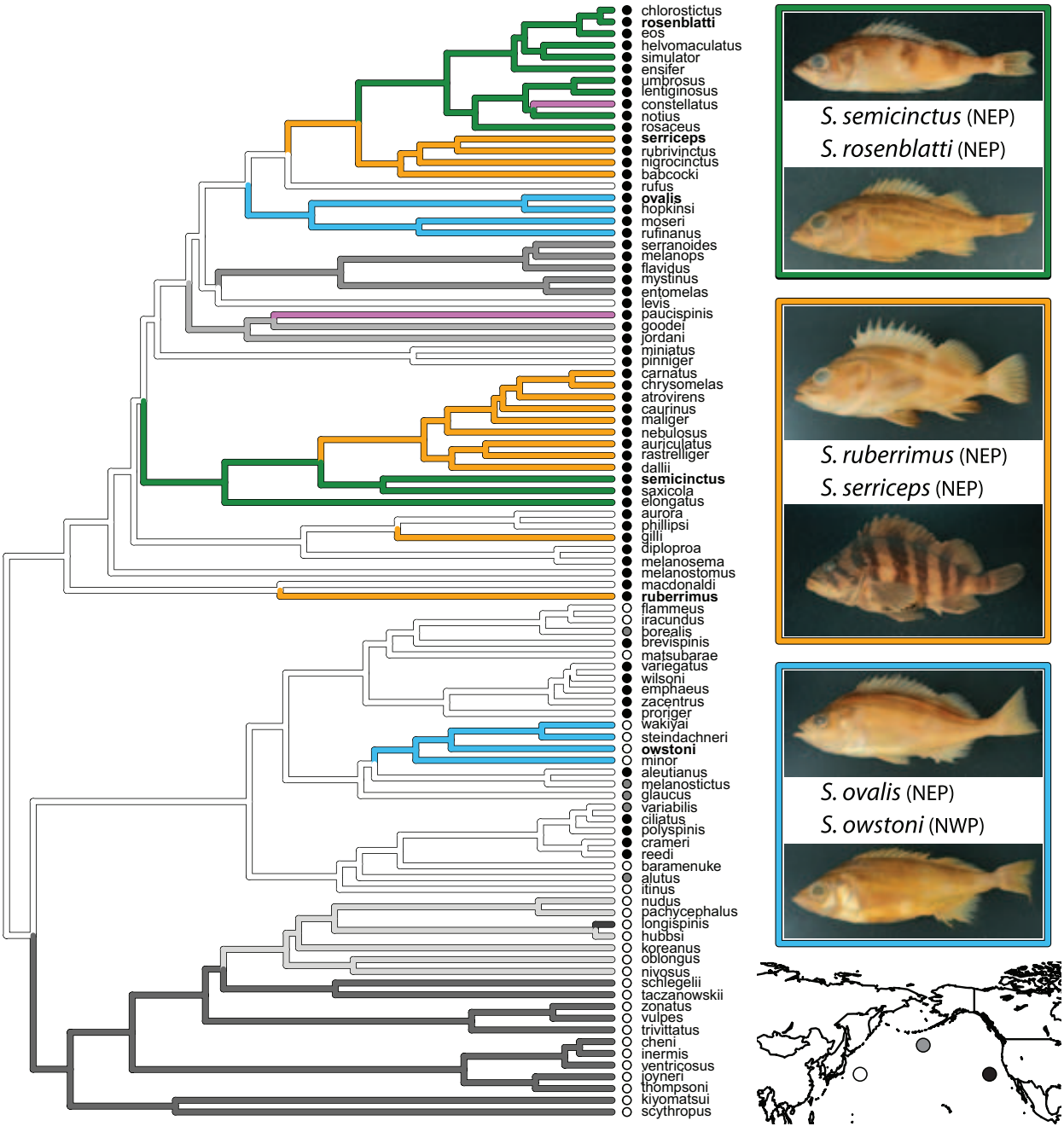

Figure 1: Maximum clade credibility (MCC) phylogeny of *Sebastes* rockfishes, depicting geographic distribution and results of the SURFACE analysis. Branch colors show regime assignments in the fitted model (white = ancestral regimes; grayscale = nonconvergent regimes; colors = convergent regimes), and circles beside species names indicate geographic regions (inset map: black = northeast Pacific [NEP]; gray = trans-Pacific; white = northwest Pacific [NWP]). Photographs show examples of species identified as belonging to three convergent regimes, two that demonstrate convergence within the NEP and one that demonstrates between-region convergence. Note that maximum total length and gill raker traits, which load most strongly on phylogenetic principal components 1 and 2, are not represented in these photos and that photos were chosen based on availability and do not represent the most convergent species pair in each regime (see fig. 3*C*, 3*D*). Photos by T. Ingram and O. L. Lau.

NEP specimens and a subset of NWP specimens, while Y. Kai measured the majority of NWP specimens; we made every effort to ensure that measurements were taken consistently by both measurers. We added published measurements for the holotype and the paratype of *Sebastes rufinanus* (Lea and Fitch 1972), which is abundant but rarely collected in the NEP, to bring the total to 95 species. Measurements included a suite of characters known or suspected to be relevant to the ecology of rockfish or other teleost fishes. These include total length (TL) as a measure of overall body size and maximum body depth and body width at the operculum as measures of body shape. Relative elongation tends to increase with depth habitat and reliance on pelagic prey in rockfish (Valentin et al. 2002; Ingram and Shurin 2009; Ingram 2011) and in fish communities in general (Neat and Campbell 2013). Pectoral fin shape (length and width) is often related to swimming speed and maneuverability (Walker and Westneat 2002; Kane and Higham 2012). The size of the eye is likely to reflect differences in sensory environment, such as depth habitat, and diurnal versus nocturnal activity (Warrant and Locket 2004; Goatley and Bellwood 2009; Ingram 2011). Traits related more directly to foraging ability are upper and lower jaw lengths, gill raker number, and longest gill raker length (Wright et al. 1983; Wainwright and Richard 1995; Carroll et al. 2004), with longer and more numerous gill rakers predictive of rockfish species feeding on smaller, low-trophic-position prey (Ingram and Shurin 2009; Ingram 2011). We averaged measurements of the left and right sides of the body for bilateral traits and natural log transformed all traits prior to analysis. Some traits could not be measured on certain specimens, but all traits were represented for all species.

To identify size-independent axes of trait variation, we calculated residual values from phylogenetic regressions of each log-transformed trait against logTL. For each trait, we first calculated species mean values, as well as species mean TL, after excluding any individuals unmeasured for that trait. We then used the function phyl.resid in the R package phytools (Revell 2012) to estimate the phylogenetically correct regression equation while simultaneously optimizing the scaling parameter λ to avoid bias due to non-Brownian evolution (Revell 2009). We used the residuals from this regression as species' size-adjusted trait values. As the specimens we were able to measure, largely collected by fishing boats or museums, were potentially nonrandom samples with regard to species' typical adult sizes, we substituted log-transformed published maximum TL values (Love et al. 2002; Froese and Pauly 2013) as a measure of body size. While maximum sizes are subject to the effects of sampling intensity and extreme observations, in taxa with indeterminate growth and no clear delineation between subadults and adults, maximum size can be a more appropriate measure of adult size than sampled body sizes (e.g., Stephens and Wiens 2009; Hendry et al. 2014).

We reduced the dimensionality of the morphological data by carrying out a phylogenetic principal components analysis (pPCA) on the covariance matrix of the species trait data (maximum TL and nine size-corrected traits) while simultaneously optimizing λ (Revell 2009, 2012). We note that one trait (gill raker number) is meristic rather than metric but that it is variable enough that species means were effectively continuous and approximately normally distributed; as for the other traits, log-transformed values can still be interpreted as proportional differences. We retained the first four axes, which had interpretable correlations with the original trait values (loadings > 0.5) and associations with ecology (see below), and cumulatively explained 93% of the variation in the data (table 1). To account for phylogenetic uncertainty in the construction of morphospace and the analyses of convergence, we repeated both the size correction and the pPCA for each of the 100 phylogenetic trees, producing 100 trait data sets. While signs of loadings were occasionally reversed, interpretation of the pPCA axes was highly similar across trees (data available on request). Data files with raw individual data, species mean residual trait values, and species pPCA scores have been deposited in the Dryad Digital Repository: http://dx.doi.org/10.5061/dryad.s5s3s (Ingram and Kai 2014).

Associations between Morphology and Ecology

To confirm relationships that have previously been identified between subsets of this morphological data set and aspects of species' ecology, we used phylogenetic multiple regression to ask whether the four pPCA axes predict two important ecological dimensions: mean trophic position

Table 1: Loadings for the first four components of the phylogenetic principal component analysis (pPCA) carried out using the maximum clade credibility phylogeny

Character	pPC1	pPC2	pPC3	pPC4
Max. total length	**.97**	.23	.04	.00
Body depth	.31	−.03	**−.59**	**−.47**
Body width	.32	−.13	**−.66**	−.19
Eye width	−.17	**.40**	**−.64**	.34
Upper jaw length	.39	−.32	**−.71**	.27
Lower jaw length	.33	−.15	**−.68**	**.45**
Gill raker no.	**−.42**	**.69**	.29	−.09
Gill raker length	**−.42**	**.89**	−.12	−.04
Pectoral fin length	−.10	−.07	−.26	−.37
Pectoral fin width	.22	−.33	**−.44**	**−.75**
Variance explained (%)	55.2	24.7	8.6	4.4

Note: Boldface indicates traits used to interpret the axes.

and adult depth habitat. We used trophic position and depth data from Ingram (2011); these data represent 44 and 66 NEP species, respectively (directly comparable data are not readily available for the NWP species). We used the pgls function in the R package caper to fit multiple regression models predicting each ecological axis from the four morphological axes (without interactions), after first removing from the tree species that lacked ecological data. We then used the MuMIn R package to calculate the Akaike's Information Criterion corrected for finite sample size (AICc) for each model nested within the full model and to calculate model-averaged parameter estimates and confidence intervals, using the subset averaging technique. We also calculated relative importance (RI) for each trait as the sum of the Akaike weights for all models containing that term (Burnham and Anderson 2002). We repeated the phylogenetic multiple regression and model averaging for each of the 100 trees and associated trait data sets and recorded for each trait the range of RI values and the frequency with which the trait was in the best-fitting model (table 2).

Table 2: Phylogenetic multiple regressions predicting rockfish ecology from morphological traits

Trait	Estimate (95% CI)	RI (95% CI_{phylo})	Trees (%)
Trophic position:			
pPC1	.53 (.22, .84)	.98 (.95, .99)	100
pPC2	−.32(−.74, .09)	.51 (.37, .71)	53
pPC3	−.08 (−.80, .64)	.24 (.23, .27)	0
pPC4	.17 (−.65, .99)	.25 (.23, .28)	0
Depth habitat:			
pPC1	1.20 (−.93, 3.32)	.38 (.34, .53)	14
pPC2	4.59 (1.24, 7.93)	.92 (.75, .98)	100
pPC3	2.24 (−3.56, 8.03)	.30 (.26, .43)	0
pPC4	9.99 (2.24, 17.75)	.89 (.81, .96)	100

Note: Trophic position is species mean trophic position, estimated from stable nitrogen isotopes relative to food web baseline values, and depth habitat is the square root transformed midpoint adult depth (data from Ingram 2011). Parameter estimates are model averaged, and relative importance (RI) sums the Akaike weights of the models containing the parameter. The 95% confidence interval (CI) for RI comes from the range of values across 100 trees from the posterior distribution, and the percentage of trees is that for which the parameter was retained in the model with the lowest corrected Akaike's Information Criterion.

Phenotypic Similarity of Rockfish Faunas

We used two statistical approaches to quantify the extent of convergence in *Sebastes*. First, we measured the morphological similarity of the rockfish faunas in the NEP and NWP to evaluate whether two faunas contain exceptionally similar sets of species (Schluter 2000). We quantified the phenotypic similarity between each pair of species as their Euclidean distance in the four-dimensional morphospace obtained from the pPCA (Ricklefs and Travis 1980) and identified for each species its nearest neighbor (with the lowest Euclidean distance) in the other region. We then calculated mean nearest neighbor distances (MNNDs) by averaging these nearest neighbor distances across all species in the NEP ($MNND_{NEP}$) and in the NWP ($MNND_{NWP}$) and then averaging these two values to obtain the mean nearest neighbor distance as an overall measure of similarity between the regions (Mahler et al. 2013). We excluded TP species that occur in both regions and would count as their own nearest neighbor, but results were qualitatively unchanged when TP species were included.

This nearest neighbor approach is appropriate for tests of clade-wide convergence between regions or for convergence between distinct clades that occur within the same region (Kozak et al. 2009; Rutschmann et al. 2011). However, in cases where we hypothesize that multiple lineages within a single clade have converged on the same parts of morphospace, an alternative method is required. Muschick et al. (2012) devised such a test based on comparing phenotypic and phylogenetic distances between species, which they used to show widespread convergence in Lake Tanganyika cichlids. This approach visualizes the pattern of trait divergence over time by plotting Euclidean distances between all pairs of species against their phylogenetic distance or the age of their most recent common ancestor. If convergence between distantly related lineages is common, this figure should contain many pairs of phylogenetically distant but phenotypically similar species in the lower right corner of the panel. Following Muschick et al. (2012), we divided this pairwise distance plot into hexagonal bins and counted the number of points in each bin. We first scaled the maximum phylogenetic distance to 1 to allow comparison among trees with different root ages and then divided this axis into six bins. We also separated the points into those representing two species in the NEP, two species in the NWP, or one species in each region, while ignoring the five TP species. This allowed us to explore between- and within-region convergence in a shared analytic framework.

To test whether either measure of convergence—the MNND or the number of points in pairwise distance bins representing convergence—exceeded the expectation by chance, we compared them to the same measures simulated under null models that lack deterministic convergence. We started with Brownian motion (BM), a standard stochastic evolutionary model in which trait evolution follows a random walk with a constant rate of nondirectional change (σ^2). We also considered a simple Ornstein-Uhlenbeck (OU) model in which stochastic evolution is combined with deterministic attraction to a single optimum θ with force α. The tendency toward the optimum

in this OU1 model has the effect of overwriting the signal of earlier evolutionary change and can produce similar species simply through constraints on trait diversification (Hansen 1997). We estimated the maximum likelihood rate parameters under each model (σ^2 for BM, σ^2 and α for OU1) separately for each trait using the ouch package in R (Butler and King 2004). We then simulated 999 data sets under each of the BM and OU1 models to generate null morphospaces to compare with the observed morphospace. We repeated this model fitting and simulation for each of the 100 trees from the posterior distribution. We also considered as an alternative null model an early burst model in which the rate of Brownian evolution declines exponentially over time (Harmon et al. 2010). We fit the early burst model to each trait using the R package geiger (ver. 1.99-4; Harmon et al. 2008), but as it received no support, we did not use it for subsequent analyses.

We used these null morphospaces to ask whether the rockfish faunas showed more convergence than expected by chance. We preserved the assignment of species to regions and compared the observed measures of convergence that incorporate geography to null distributions. We calculated the one-tailed significance of the nearest neighbor statistic as the proportion of null MNND values less than or equal to the observed value. For the pairwise distance analysis, we compared the number of points in each hexagonal bin to the distributions obtained after repeating the binning procedure on the data sets simulated under BM and OU1. We compared values to both the 2.5th and 97.5th percentiles of the null distributions, as we might expect a significant excess of points in some bins to be associated with a significant deficit of points in other bins. If the data contain significantly more points in the bins representing phenotypically similar but phylogenetically distant species, then this indicates a greater degree of convergence than expected by chance. We repeated these analyses for each of the 100 trees and associated data sets; we report the proportion of significant tests across all trees to evaluate the sensitivity of results to phylogenetic uncertainty.

Macroevolutionary Models of Convergent Peak Shifts

To evaluate whether any phenotypic similarity in rockfish can be explained by lineages converging on the same adaptive peaks, we used the recently developed comparative method SURFACE (Ingram and Mahler 2013; Mahler and Ingram 2014). SURFACE uses a stepwise AIC routine (Alfaro et al. 2009; Thomas and Freckleton 2012) to fit Hansen models: OU models with multiple optima in which shifts between evolutionary regimes are "painted" onto the branches of a phylogenetic tree (Hansen 1997; Butler and King 2004; Beaulieu et al. 2012). A novel feature of this method is that by taking as input only the phylogeny and multidimensional phenotypic data, it can identify cases of convergence across a clade while avoiding potential biases associated with the subjective a priori designations of candidate convergent taxa. While this approach does not estimate an adaptive landscape per se (i.e., the relationship between fitness and trait values across the entire trait space), Hansen models can be interpreted as representing shifts between adaptive peaks (Hansen 1997, 2012), and the ability of SURFACE to recover such models without a priori specification of peak shifts make it the best current approach to recovering macroevolutionary adaptive landscapes from comparative data. We refer to peak shifts on a macroevolutionary adaptive landscape in what follows, but the models can also be interpreted as shifts between evolutionary regimes without assuming a landscape.

SURFACE consists of a "forward" stepwise phase, in which peak shifts are added to the tree, followed by a "backward" phase, which identifies shifts that are toward the same peaks (for a detailed explanation and discussion of statistical performance, see Ingram and Mahler 2013). The starting point is the OU1 model fit in ouch, with maximum likelihood used to estimate σ^2, α, and θ for each of the $m = 4$ traits. The four log likelihoods are added, under the assumption that σ^2 and α are uncorrelated across traits and used to calculate the AICc. The AICc balances model fit (likelihood) against complexity (number of parameters) while accounting for finite sample size. For our purposes, the sample size is equal to m times the number of species (95), and the number of parameters is $p = k + m(k' + 2)$. Term k is the number of peak shifts, counting an ancestral shift at the base of the clade, and k' is the number of peaks. Peak shifts apply to all traits, while term $m(k' + 2)$ accounts for estimates of each of the k' optima, plus an estimate of σ^2 and α for each trait. Each step of the forward phase of SURFACE adds one new shift to a new peak (optimum), resulting in a more complex Hansen model (with k and k' both increasing by one). For each branch of the tree, a candidate model is generated by adding a peak shift that affects that branch and its descendant branches. The AICc of each candidate model is calculated by adding log likelihoods as before, and a peak shift is placed on whichever branch, if any, provides the greatest improvement (decrease in AICc) over the previous model. This shift is retained in subsequent models, and the process of adding peaks is iterated until the AICc ceases to improve.

The Hansen model returned by the forward phase has k peak shifts on the tree, each toward a unique peak represented by an optimum for each trait. The backward phase tests whether the model improves further if groups of peaks are collapsed into $k' < k$ convergent peaks. Collapsing a pair of peaks can improve the AICc because it

decreases the number of optima estimated (by m), thus simplifying the inferred adaptive landscape while the number of shifts remains the same. Candidate models are generated by collapsing one pair of peaks at a time into a single convergent peak. Pairwise collapses that improve the AICc are incorporated into the model, with a clustering algorithm used to identify clusters of peaks that can be collapsed without conflict (Ingram and Mahler 2013). This second stepwise process is iterated, with additional peak shifts potentially being incorporated into previously collapsed peaks, until the AICc again stops improving. The difference in AICc between the models returned by the forward and backward phases, $\Delta\text{AICc}_{\text{conv}}$, provides an indication of how much accounting for convergence improved overall model performance. The change in AICc throughout the analysis can also be visualized and partitioned among traits to examine how much each trait contributed to the model fit (Mahler and Ingram 2014).

The final model identified by SURFACE has k shifts to $k' \leq k$ adaptive peaks. The extent of convergence in this model can be quantified using Δk, the extent to which accounting for convergence simplifies the adaptive landscape by reducing the number of peaks: $\Delta k = k - k'$. We also report an alternative measure, the number of cases of convergence cc (note that this differs from the statistic c described in Ingram and Mahler 2013). Cases of convergence cc is the number of pairs of peak shifts that are to the same peak: where n is a vector of the number of shifts per peak,

$$cc = \sum \binom{n}{2}.$$

For example, a peak that was reached by two shifts features a single case of convergence ($cc = 1$), while for a peak reached by three shifts, $cc = 3$ (pairwise combinations of shifts 1–2, 1–3, and 2–3). The advantage of this measure is that it allows each case of pairwise convergence to be assigned to a category based on its geographic context, so that cc can be partitioned into within-region and between-region convergences (Mahler and Ingram 2014).

We reconstructed the ancestral geography of lineages that underwent peak shifts using stochastic character mapping (Huelsenbeck et al. 2003), treating geography as a binary state (NEP or NWP). Rather than treat the five TP species as a separate category, we accounted for the ambiguity in their region by randomly assigning the region of each TP species as either NEP or NWP prior to generating each geographic history. We generated 100 histories for the MCC tree using the function make.simmap in the R package phytools (Revell 2012). We classified the geography of each branch that contained a peak shift in the Hansen model based on whether the reconstruction placed the end of the branch in the NEP or the NWP. While the peak shift placed by SURFACE is constrained to occur at the beginning of the branch, transitions in stochastic character maps can occur at any point, so the most appropriate comparison is whether the branch includes a shift or not (Mahler and Ingram 2014). We classified each case of pairwise convergence based on the geographic status of the two branches and counted the number of between-region cases (cc_{TP}) that involved one lineage in each region and the number of within-region cases with both lineages in the NEP (cc_{NEP}) or NWP (cc_{NWP}). We averaged these values across the 100 stochastic character maps to account for cases in which the geographic location of peak shifts was ambiguous.

We used a null model approach to test whether any measure of convergence (Δk, cc, cc_{NEP}, cc_{NWP}, or cc_{TP}) was greater than expected by chance. This is necessary because SURFACE may fit some number of shifts to data generated under a model that lacks convergence (Ingram and Mahler 2013). We used three null models that lack deterministic convergence: BM, OU1, and a nonconvergent Hansen null model. The latter model is derived from the final step of the forward phase of SURFACE and accounts for both the presence of peak shifts and the extent of variation among optima, while breaking up any tendency for optima to cluster in trait space beyond a random expectation. For each simulation under the Hansen null model, the optima θ are resampled from normal distributions, with the mean and standard deviation of the optima estimated from the final step of the forward stage of SURFACE (Ingram and Mahler 2013). We calculated this mean and standard deviation after excluding one outlier optimum (>3 standard deviations from the mean) that would have inflated the variances in simulated data sets. We ran SURFACE on 99 data sets simulated on the MCC tree under each of the three null models and recalculated the measures of convergence for each analysis. We infer a significantly greater extent of convergence than expected by chance if fewer than 5% of the null values of the statistic meet or exceed the observed value. Simulations assessing the power to recover a true $\Delta k > 0$ indicate that this test has good power to detect nonrandom convergence given a moderately sized tree (at least 64 taxa) and data for multiple traits (Ingram and Mahler 2013).

Estimating uncertainty in the measures of convergence in the final Hansen model is complicated by the dependence of SURFACE on a stepwise algorithm and a single tree topology. Confidence intervals can be obtained for the parameters describing the evolutionary process using a parametric bootstrap approach (Butler and King 2004), simulating under and then reestimating the fitted Hansen model many times, but this does not reveal uncertainty in the broader convergence parameters. We used a related bootstrap approach in which we simulated data sets under

the fitted Hansen model and ran SURFACE on the simulated data sets, allowing us to recalculate all convergence parameters. We also incorporated phylogenetic uncertainty by first running SURFACE on each of the 100 trees from the posterior distribution and calculating convergence parameters for each (generating 100 stochastic character maps per tree for the geographic parameters). We also obtained a total of 500 bootstrap estimates of the convergence parameters by running SURFACE on five data sets simulated under each of the 100 fitted Hansen models.

Results

Phylogeny Reconstruction

The phylogeny that resulted from the BEAST analysis was generally consistent with previous estimates of the *Sebastes* tree (Hyde and Vetter 2007), including the recovery of a clade of 51 species exclusive to the NEP (ignoring lineages that dispersed to the Southern Hemisphere and the Gulf of California) and a clade of 19 species exclusive to the NWP (figs. 1, A1). The early divergences differ somewhat from Hyde and Vetter's (2007) tree, but we nonetheless corroborate earlier findings that dispersal between regions is relatively rare and that substantial clades are endemic to one region or the other. After pruning to exclude non-*Sebastes* outgroups, the MCC tree had a root age of 8.35 Myr, with a range of 8.00–10.35 Myr across the 100 trees.

Morphospace Construction

Rockfish maximum total length varies over almost an order of magnitude, from *Sebastes rufinanus* at 17 cm to *Sebastes borealis* at 108 cm (Love et al. 2002; Froese and Pauly 2013). The pPCA revealed major axes of trait variation generally similar to a previous study that used a subset of the present data (Ingram and Shurin 2009): pPC1 had strong positive loadings with maximum TL and weaker negative loadings with gill raker length and gill raker number; pPC2 loaded positively with gill raker number and length and, to a lesser extent, with eye width; pPC3 loaded negatively with body width and depth, eye width, jaw length, and pectoral fin width; and pPC4 loaded negatively with pectoral fin width and body depth and positively with lower jaw length. The pPCA axes 1–4 explained 55.2%, 24.7%, 8.6%, and 4.4% of the variation in morphology among species, respectively, for a total of 92.9% of morphological variance explained (table 1).

Associations between Morphology and Ecology

As previously demonstrated (Ingram 2011), several morphological traits are associated with mean trophic position and adult depth habitat in NEP rockfish (table 2). Trophic position was consistently associated with pPC1 (RI = 0.98), with higher trophic positions associated with larger body size and shorter and less numerous gill rakers. Corresponding to gill raker number and length, pPC2 showed a weaker, negative association with trophic position (RI = 0.51), which was included in the preferred model for approximately half of the trees. Depth habitat was positively associated with both pPC2 (RI = 0.92) and pPC4 (RI = 0.89), both of which were retained in the preferred model for all 100 trees. Deeper habitats were associated with longer, more numerous gill rakers and larger eyes (pPC2) as well as with narrower bodies and pectoral fins and longer jaws (pPC4). These results are broadly consistent with a trait-by-trait analysis of NEP rockfish morphology-ecology associations using this data set (Ingram 2011).

Phenotypic Similarity of Rockfish Faunas

The BM model was moderately favored over the OU1 model when evidence was weighed across traits (ΔAICc = 4.5), as well as for each trait considered individually (pPC1: ΔAICc = 0.25; pPC2: ΔAICc = 5.3; pPC3: ΔAICc = 4.3; pPC4: ΔAICc = 1.3). However, as the magnitude of the difference was relatively small for some traits, and as the OU1 model was favored over BM for 60 of 100 trees from the posterior distribution, we use both BM and OU1 as null models in the analyses that follow. The early burst model was never supported (in each case, the estimate of the rate decline parameter was zero, so it reduced to BM), and we therefore did not give it further consideration.

Rockfish from the NEP and NWP occupied similar regions of morphospace, with a few exceptions (see "Discussion"; fig. 2*A*–2*C*). The mean nearest neighbor distance in morphospace between species and their closest counterparts in the opposite region was lower than expected under a Brownian motion null model, indicating significant faunal similarity (fig. A2; MNND = 0.28, $P = .021$). This result was driven by a strong tendency for NEP species to have more similar species in the NWP than expected by chance ($\text{MNND}_{\text{NEP}} = 0.27$, $P = .002$), whereas NWP species did not have more similar NEP species than expected ($\text{MNND}_{\text{NWP}} = 0.29$, $P = .21$). Compared to the OU1 model, the degree of matching was no longer greater than expected by chance overall ($P = .45$), although it still approached significance for MNND_{NEP} ($P = .075$). These results were consistent across trees, with the overall MNND significantly smaller than expected ($P < .05$) for all 100 of the trees when using the BM null model but for none of the 100 trees when using the OU1 model. The results were similar for MNND_{NEP} (BM: significant for 100 of 100 trees; OU1: significant for 1 of 100 trees).

Pairwise distance contrasts also revealed morphological

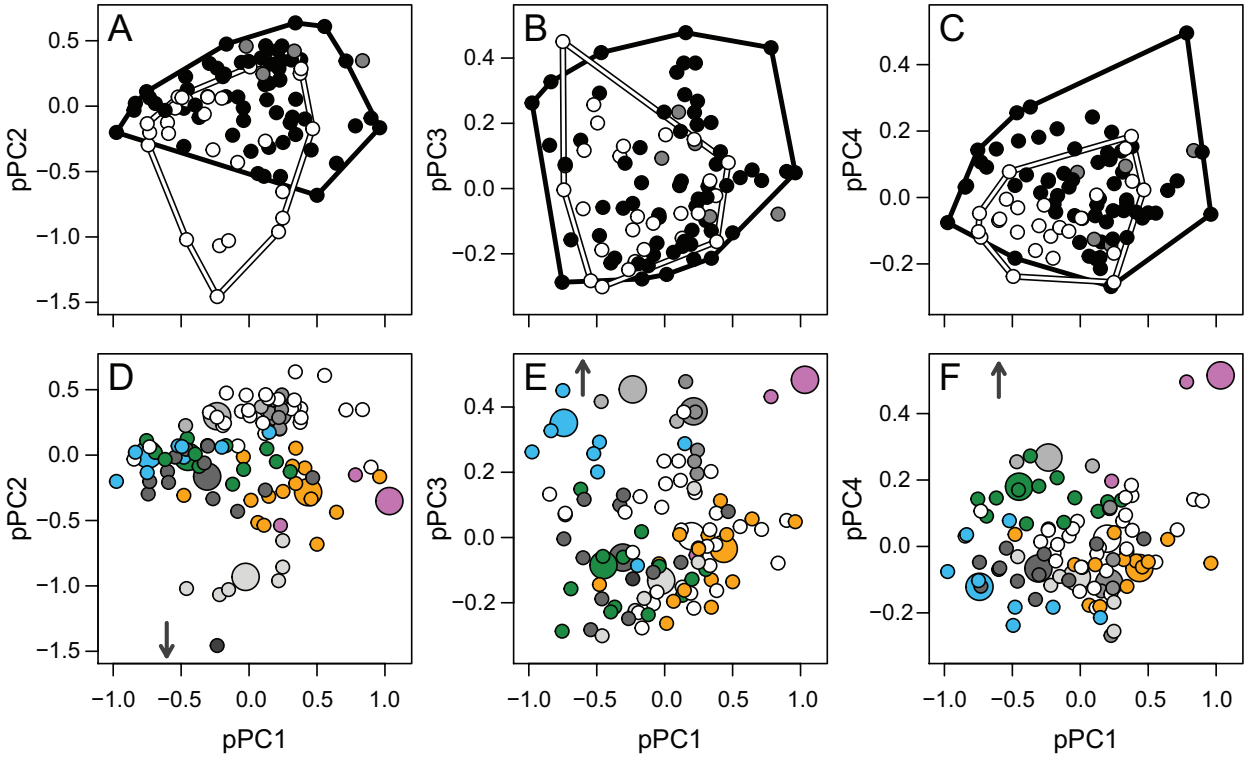

Figure 2: *A–C*, Convex hulls illustrating the volume of morphospace occupied by *Sebastes* species in the northeast Pacific (black outlines) and northwest Pacific (white outlines). Trans-Pacific species are indicated by gray circles and are not included in either convex hull. *D–F*, Positions of optima inferred by SURFACE in morphospace (large circles) compared to species mean trait values as in *A–C* (small circles). Color represents convergent regimes, and grayscale represents nonconvergent regimes in the fitted Hansen model (see also fig. 1). The position of one optimum, which is outside the range of the trait data for phylogenetic principal components 2–4 (pPC2–pPC4), is indicated by arrows.

similarity of species in different regions and within the NEP (fig. 3). Hexagonal bins representing low morphological distance and high phylogenetic distance were generally overrepresented compared to the expectation under the BM null model, and in some cases, the observed values fell above the 97.5th percentile of the null distribution (fig. 3*B*–3*D*, red cells and black asterisks at lower right). There was also a tendency toward an overrepresentation of morphologically divergent close relatives, while cells corresponding to highly divergent distant relatives and to highly similar close relatives tended to be underrepresented relative to BM. As with the MNND analysis, these results were no longer exceptional when compared to the OU1 model (fig. A3). Across 100 trees, these patterns were again similar: compared to the BM null model, bins representing convergence were often significantly overrepresented in the pairwise distance plots between regions and within the NEP but not within the NWP or compared to the OU1 null model.

Macroevolutionary Models of Convergent Peak Shifts

The Hansen model returned by the SURFACE analysis of the MCC tree included $k = 16$ peak shifts and a total of $k' = 10$ peaks, 5 of which were reached by multiple peak shifts (figs. 1, 2; table 3). The measures of convergence were $\Delta k = 6$, based on the extent of simplification of the inferred adaptive landscape ($k - k'$), and $cc = 9$, based on the number of pairs of convergent peak shifts. The AICc improved by 82.5 units during the forward phase and by another 49.4 units during the backward phase. By far, the largest contribution to the AICc improvement came from pPC2, with a moderate contribution from pPC4 and little contribution from pPC1 or pPC3 (fig. 4). Estimates of the attraction parameter α ranged from 0.32 to 2.02 across traits; converted to the more intuitive phylogenetic half-life ($t_{1/2}$), this corresponds to expected times of 0.34–2.11 Myr to evolve halfway toward an optimum (table A1, available online).

While this result implies a number of convergent peak

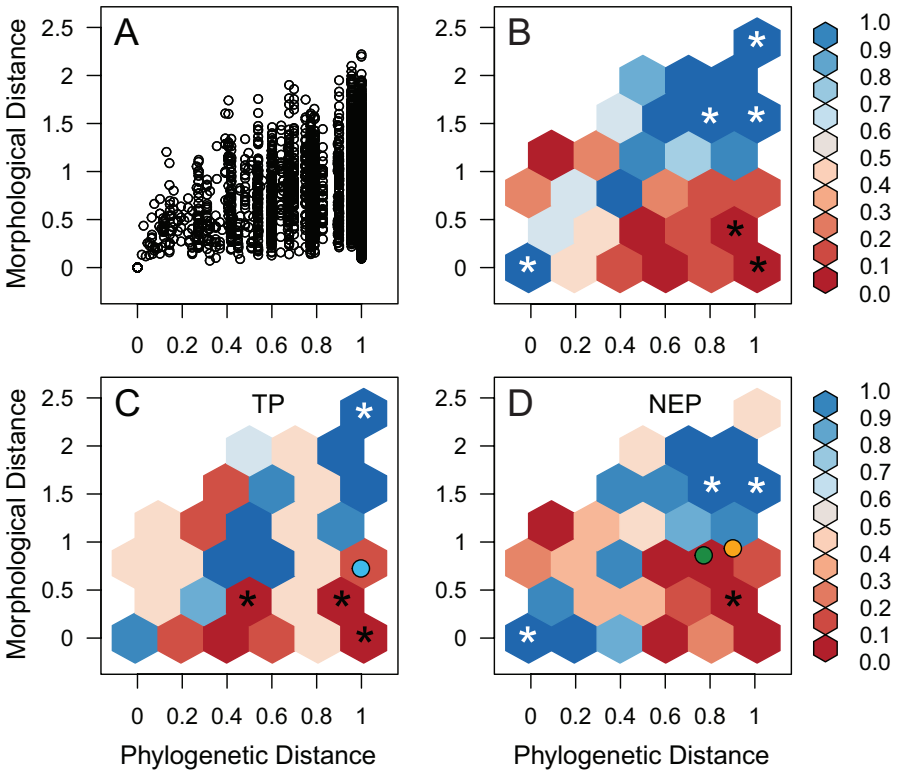

Figure 3: Morphological and phylogenetic distances between rockfish species. *A*, All pairwise distances between species. *B*, Proportion of Brownian motion (BM) simulations in which the number of pairs falling into each hexagonal bin exceeds the observed data, where red colors indicate bins containing more pairs in the observed data than expected. Asterisks indicate bins where the density falls outside the 95% confidence interval expected under BM. *C*, *D*, As above but separated into pairwise distance contrasts between northeast Pacific (NEP) and northwest Pacific (NWP) species (trans-Pacific [TP]; *C*) and between NEP species only (*D*), with the positions of the species illustrated in figure 1 depicted with colored symbols.

shifts in North Pacific *Sebastes*, most of this convergence occurred within the NEP rather than between regions. By combining the shift positions in the tree inferred by SURFACE with the biogeographic histories generated with stochastic character mapping, we obtained estimates of $cc_{NEP} = 8.0$ convergent shifts occurring within the NEP, compared to $cc_{NWP} = 0.0$ within the NWP and $cc_{TP} = 1.0$ case of between-region convergence.

The number of peak shifts $k = 16$ in the model fitted to the rockfish data was somewhat larger than expected under BM (mean $k_{null} = 10.8$, $P = .09$) and significantly greater than expected under the OU1 null model (mean $k_{null} = 8.7$, $P = .02$), while the nonconvergent Hansen null model successfully accounted for the observed number of peak shifts (mean $k_{null} = 15.6$, $P = .50$). The extent of convergence was higher than expected by chance, reaching significance for some but not all combinations of convergence parameter and null model. Evidence for convergence greater than expected was slightly stronger for *cc* (BM null model: $P = .05$; OU1: $P = .03$; nonconvergent Hansen: $P = .05$) than for Δk (BM: $P = .09$; OU1: $P = .05$; nonconvergent Hansen: $P = .19$). The number of cases of between-region convergence did not differ from the null expectation, while the number of cases within the NEP was higher than under any null model (all $P = .02$). The extent to which the model performance improved during the backward phase of SURFACE, $\Delta AICc_{conv}$, was also greater than expected under the null models (BM: $P = .01$; OU1: $P = .01$; nonconvergent Hansen: $P = .05$). Examination of 95% confidence intervals obtained via parametric bootstrapping on the MCC tree yielded conclusions similar to the results of the null model tests (table 3).

Results of the SURFACE analysis varied across the sample of trees from the posterior distribution. Measured as the proportion of pairs of species whose regime assignment (same vs. different regimes) is consistent between trees (Ingram and Mahler 2013), the pairwise similarity of the SURFACE fit between trees averaged 90% (range 62%–100%). When phylogenetic uncertainty was incorporated

into the parametric bootstrap simulations, the 95% confidence intervals around the convergence parameter estimates were generally similar to those obtained for the MCC tree. However, the fact that SURFACE inferred substantially less convergence for a subset of trees meant that while the intervals for Δk and *cc* excluded zero, the interval for cc_{NEP} did not (table 3; fig. A4). By comparing the frequency with which each pair of species was assigned to the same regime across 100 trees, we could identify those lineages that were consistently identified as convergent and those where the support for convergent peak shifts varied with the topology of the tree (fig. A5).

Discussion

Sebastes rockfish lineages have evolved convergent morphology multiple times as they have radiated throughout the North Pacific. While we did find some evidence that the radiations in the NEP and NWP are partly replicated, we found stronger support for a history of convergent adaptive evolution among lineages within the NEP.

The rockfish faunas in the NEP and NWP showed greater similarity to one another (i.e., lower mean nearest neighbor distance in morphospace) than expected under a Brownian motion null model. Interestingly, the extent of matching was asymmetric: NEP species tend to have close counterparts in the NWP, while NWP species did not have more similar species in the NEP than expected. This asymmetry may result from differences between regions in the occupancy of morphospace (see below). The statistical similarity of the sets of phenotypes in the two faunas may be attributed either to deterministic convergence or to chance similarity resulting from stochastic evolution in a low-dimensional or constrained trait space (Stayton 2008). In fact, we found that the degree of matching did not exceed the expectation under an OU1 model, although the result still approached significance for the NEP. These results were generally corroborated by the pairwise contrast approach, which showed more convergent pairs of species in different regions than expected under the BM null model but not under the OU1 null model.

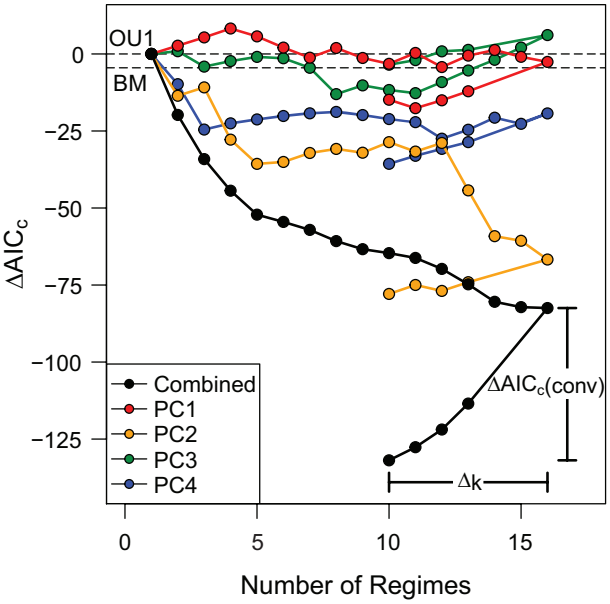

Figure 4: Change in the corrected Akaike's Information Criterion (AICc) during the forward (left-to-right) and backward (right-to-left) phases of SURFACE analysis. The black line shows the overall improvement in the AICc at each step, and the colored lines show the partial AIC ($-2 \log L$ plus one-quarter of the penalty, scaled to an initial AICc of zero) for each of the four traits, demonstrating the contribution of each trait to the overall improvement in the AICc. The dashed lines indicate the AICc for the Ornstein-Uhlenbeck 1 (OU1) and Brownian motion (BM) models; Δk and $\Delta AICc_{conv}$, the difference in corrected Akaike's Information Criterion between models, are indicated to facilitate interpretation of table 3.

Table 3: Results of the SURFACE analysis of rockfish data using the maximum clade credibility (MCC) phylogeny and comparisons to three null models

Parameter	Estimate	95% CI_{MCC}	95% CI_{phylo}	p(BM)	p(OU1)	$p(H_{NC})$
No. shifts (*k*)	16	11.5–20	10–20	.09	.02	.50
Convergence (Δk)	6	2–8.5	1–8	.09	.05	.19
Pairwise cases (*cc*)	9	2–13.5	1–11	.05	.03	.05
cc_{TP}	1.0	0–4.9	0–5	.71	.67	.74
cc_{NEP}	8.0	1–9.5	0–8.5	.01	.01	.02
cc_{NWP}	.0	0–1	0–1	1.00	1.00	1.00
$\Delta AICc_{conv}$	49.4	13.4–66.2	4.2–63.9	.01	.01	.05

Note: Here, CI_{MCC} is the approximate 95% confidence interval from 100 parametric bootstraps of the maximum clade credibility (MCC) tree, and CI_{phylo} is from 5 bootstraps for each of the 100 trees. *P* values are the proportion of values greater than or equal to the MCC estimate (which is included in both numerator and denominator) after running SURFACE on 99 data sets simulated under each null model. BM = Brownian motion; OU = Ornstein-Uhlenbeck; H_{NC} = nonconvergent Hansen; TP = trans-Pacific; NEP = northeast Pacific; NWP = northwest Pacific; ΔAICc = difference in corrected Akaike's Information Criterion between models.

While the BM model was favored over OU1, at least for the MCC tree, the fact that a model that imposes constraints on trait space can account for the observed statistical similarity precludes us from confidently inferring cladewide convergence between regions and makes it important to consider the fit of alternative explanatory models.

Our analysis using SURFACE places the statistical patterns of the nearest neighbor and pairwise contrast analyses into a mechanistic framework by incorporating a process that can result in convergence: adaptation to multiple adaptive peaks. We found that models with convergent peak shifts strongly outperformed nonconvergent models and that measures of convergence generally exceeded the expectation under the BM, OU1, or Hansen null model that accounted for the presence of nonconvergent peak shifts. To the extent that the positions of optimum trait values in Hansen models can be interpreted as adaptive peaks, this suggests that morphological diversification in rockfish is better described by evolution on a Simpsonian macroevolutionary landscape than by stochastic evolution, where any convergence results from constraints on trait space. Traits varied in the extent to which they contributed to the fit of the model. Model improvement as peaks were added in the first phase of SURFACE was dictated largely by improvement to the likelihood for pPC2 (gill raker number and length) and, to a lesser extent, pPC4, while all traits contributed during the second phase in which convergent peaks were identified. Gill raker number and length are strongly associated with dietary niche in NEP rockfish (Ingram and Shurin 2009; Ingram 2011), although pPC2 was not as strongly associated with trophic position as pPC1, which loaded on body size as well as gill rakers. Both pPC2 and pPC4 predicted depth habitat in NEP rockfish, suggesting that the morphological traits that showed support for convergent peak shifts have ties to both trophic ecology and habitat (table 2).

The results of the SURFACE analysis should be considered in light of several caveats associated with this approach. This method takes advantage of stepwise AICc as a computationally tractable way to explore parameter space (Alfaro et al. 2009), but this makes the final model dependent on the order in which peak shifts and cases of convergence are added. This can make the inferred Hansen model sensitive to the tree topology, as indicated by the variation in measures of convergence across the posterior distribution of trees (fig. A4). SURFACE makes the simplifying assumptions that the rates of stochastic evolution σ^2 and adaptation α are constant across the tree and that these parameters do not covary between traits. Violations of the constant-α assumption can lead to inference of optima quite distant from species trait values, and we found that one optimum (estimated for a peak occupied only by *Sebastes longispinis*) fell well outside the range of PC2–PC4 (fig. 2*D*–D*F*). Models that allow heterogeneity in α and σ^2 among peaks are now available (Beaulieu et al. 2012) but have yet to be combined with approaches that identify the positions of peak shifts, and it may not prove possible to distinguish among alternative models (e.g., change in the optimum, α or σ^2) for very small subclades. The assumption of independence of the evolutionary parameters among traits is likely to be at least approximately valid given that the morphospace was obtained from a phylogenetic PCA, although this procedure only ensures that the axes are orthogonal under the λ transformation of the BM model. While true multivariate methods for fitting OU models are becoming available (Bartoszek et al. 2012), they are not currently integrated with an algorithm that can identify peak shifts.

By combining SURFACE's reconstructed history of peak shifts with the inference of ancestral geography using stochastic character mapping, we were able to estimate the extent of within- and between-region convergence. SURFACE identified only a single case of convergence between lineages in the NEP and NWP, involving the pelagic clades containing *Sebastes ovalis* (NEP) and *Sebastes owstoni* (NWP). A few other cases of between-region convergence were occasionally identified across the sample of trees (fig. A4; e.g., block of gray squares in the lower center of fig. A5 representing benthic clades in both regions), but there was no support for exceptional between-region convergence. This is somewhat surprising given that unrelated lineages in each region were once grouped together on the basis of morphology, although these groupings were based in part on traits such as head spination that were not measured here and are of unknown ecological function. In general, NWP lineages were rarely identified as convergent, with no evidence for within-NWP convergence and weak evidence for between-region convergence.

Instead of replicated radiation, we found the somewhat surprising result that convergence within the NEP was rather common, with eight cases of convergence between NEP lineages in the SURFACE result for the MCC tree. These included four benthic lineages that occur in relatively shallow habitats: *Sebastes ruberrimus*, *Sebastes gilli*, and the named subclades *Sebastichthyes* (including *Sebastes serriceps*) and *Pteropodus* (including *Sebastes caurinus*). Additionally, deeper-living and generally smaller-bodied lineages including *Sebastes semicinctus* and *Sebastes rosenblatti* were identified as sharing an adaptive peak, as were the less obviously similar *Sebastes constellatus* and *Sebastes paucispinis*. The identity of the convergent lineages varied across the distribution of trees, but convergence within the NEP was generally supported. The SURFACE results are consistent with the pairwise distance analysis, which showed an excess of morphologically similar but distantly related pairs of species in the NEP compared to the ex-

pectation under BM but not in the NWP. In combination with the SURFACE results and the asymmetry in the nearest neighbor analysis, where NWP species less frequently had a counterpart in the NEP than vice versa, this suggests that the regions differ in their tendency to reach convergent adaptive peaks.

Environmental differences between the northeast and northwest Pacific may account for the observed differences in the extent of convergence. The NEP and NWP rockfish faunas show some differences in their occupancy of morphospace (fig. 2). Several related species in the NWP (especially *Sebastes hubbsi*, *Sebastes koreanus*, *Sebastes longispinis*, and *Sebastes nudus*) occupy a region of trait space with no counterpart in the NEP, corresponding to small maximum TL and few, short gill rakers (average pPC1 and very low pPC2; fig. 2*A*). This specialist benthic phenotype is associated with the use of sea grasses as habitat by adult individuals, whereas in the NEP, sea grasses are used primarily as nursery habitats following the recruitment of juvenile rockfish from their pelagic larval phase. The NEP contains multiple benthic lineages as discussed above, but these tend to be larger bodied or use deeper habitats. The specialist NWP phenotype appears highly derived relative to the inferred ancestral peak representing pelagic species with long, numerous gill rakers such as *Sebastes pinniger* (although the caveats associated with the stepwise algorithm also limit our confidence in ancestral peaks identified by SURFACE). Otherwise, NWP rockfish generally occupy a subset of the morphospace occupied by the more diverse NEP fauna (fig. 1*A*–1*C*). Differences in the disparity and extent of convergence between regions may arise in part from variation in the diversity and abundance of potential competitors. The NWP contains representatives of the three genera most closely related to *Sebastes* (*Helicolenus*, *Hozukius*, and *Sebastiscus*), all of which are absent from the NEP. Further, ecologically similar species such as groupers (e.g., *Epinephelus* spp.) are more abundant and diverse in the NWP than in the NEP (Froese and Pauly 2013). Ecological opportunity for rockfish may thus have been greater in the NEP than in the NWP, with lineages free to undergo more frequent niche shifts that resulted in convergence in morphospace.

These results provide an interesting contrast to a recent study that used a similar set of analyses to investigate convergence in Greater Antillean anole lizards (*Anolis* sp.). Mahler et al. (2013) confirmed that *Anolis* radiations are strongly replicated across islands and showed that this faunal similarity is best explained by a history of frequent shifts between shared adaptive peaks that loosely correspond to microhabitat specialist "ecomorphs" (Losos et al. 1998). In contrast, within-island convergence is rare: the same ecomorph rarely evolves more than once on an island (Mahler and Ingram 2014), and the rate of trait evolution consequently slows down as niche space on an island becomes saturated (Mahler et al. 2010). This pattern contrasts with NEP rockfish, which show no signs of a slowdown in evolutionary rates, consistent with the continued occurrence of peak shifts in this region. It is unknown why certain traits show evolutionary slowdowns while others do not (Harmon et al. 2010), but one possibility is that characteristics involved in trophic interactions or macrohabitat preference are governed by a more dynamic adaptive landscape. The traits showing both evolutionary slowdowns and convergence in anoles (size and relative limb length; Mahler et al. 2010; Mahler and Ingram 2014) relate primarily to structural microhabitats (e.g., perch height and diameter), the distribution of which may be relatively constant. In contrast, the rockfish traits analyzed here, which relate to diet and depth macrohabitat, and measures of climatic macrohabitat in anoles (Hertz et al. 2013) do not show evolutionary slowdowns. In rockfish, divergence on the depth gradient appears to be particularly important for within-region speciation (Hyde et al. 2008; Ingram 2011; Muto et al. 2013; Venerus et al. 2013); if this divergence is driven in part by competition within species, it may facilitate shifts even to niches already occupied by more distantly related lineages in the same region. The possibility that taxa, traits, and niche axes may differ predictably in the tempo of their diversification is intriguing and warrants further theoretical and empirical investigation.

The replicated evolution of similar phenotypes in different regions has long been taken as strong evidence for the ability of natural selection to shape organisms to their environments. We found only limited evidence for convergence between the largely independent radiations of *Sebastes* in the northeast and northwest Pacific, suggesting either that morphological diversification is not governed by adaptive processes or that the regions are not sufficiently similar to produce matched sets of species. Instead, we found that most cases of convergence occurred within the northeast Pacific, the region where rockfish have diversified most extensively. The possibility of replicated or parallel adaptive radiation within regions has recently received attention in several systems (Kozak et al. 2009; Rutschmann et al. 2011; Muschick et al. 2012; Frédérich et al. 2013). It is not immediately clear why lineages occurring in broad sympatry would show such convergence, as we might expect niche incumbency to limit diversification into niches already occupied by another lineage's (Algar et al. 2012), unless the lineages had diverged sufficiently in additional, unmeasured ecological dimensions. If this diversification occurred during periods when clades were isolated from one another, the implication is that species interactions do not limit the clades from expanding to occupy the same geographic ranges (Wiens 2011). Some

theory has recently begun to explain the conditions under which interacting species may evolve to be more similar rather than more different and how such similar sets of species may emerge either in sympatry or in allopatry (Scheffer and van Nes 2006). Whether this process or differentiation in niche dimensions not associated with the traits studied here explains the convergence of rockfish lineages within the NEP remains to be seen.

The analyses we describe here indicate that convergent shifts between adaptive peaks are a feature of morphological evolution in *Sebastes* radiations, with some indication of clade-wide convergence within the northeast Pacific. Rockfish provide an example of widespread within-region convergence in a marine environment and highlight the ability of macroevolutionary models to reveal the dynamics of convergence in adaptive radiations.

Acknowledgments

T.I. was funded by postgraduate and postdoctoral awards from the National Science and Engineering Research Council of Canada. We thank H. Imamura, T. Kawai, M. Love, K. Maslenikov, M. McCrea, K. Sakai, H. J. Walker, M. Yabe, and K. L. Yamanaka for arranging access to rockfish specimens and J. B. Losos, D. L. Mahler, and two reviewers for helpful comments that improved the manuscript.

Literature Cited

Alfaro, M. E., F. Santini, C. Brock, H. Alamillo, A. Dornburg, D. L. Rabosky, G. Carnevale, and L. J. Harmon. 2009. Nine exceptional radiations plus high turnover explain species diversity in jawed vertebrates. Proceedings of the National Academy of Sciences of the USA 106:13410–13414.

Algar, A. C., D. L. Mahler, R. E. Glor, and J. B. Losos. 2012. Niche incumbency, dispersal limitation and climate shape geographical distributions in a species-rich island adaptive radiation. Global Ecology and Biogeography 22:391–402.

Barsukov, V. V. 1981. A brief review of the subfamily Sebastinae. Journal of Ichthyology 21:1–26.

Bartoszek, K., J. Pienaar, P. Mostad, S. Andersson, and T. F. Hansen. 2012. A phylogenetic comparative method for studying multivariate adaptation. Journal of Theoretical Biology 314:204–215.

Beaulieu, J. M., D.-C. Jhwueng, C. Boettiger, and B. C. O'Meara. 2012. Modeling stabilizing selection: expanding the Ornstein-Uhlenbeck model of adaptive evolution. Evolution 66:2369–2383.

Burnham, K. P., and D. R. Anderson. 2002. Model selection and multimodel inference: a practical information-theoretic approach. 2nd ed. Springer, New York.

Butler, M. A., and A. A. King. 2004. Phylogenetic comparative analysis: a modeling approach for adaptive evolution. American Naturalist 164:683–695.

Carroll, A. M., P. C. Wainwright, and S. H. Huskey. 2004. Morphology predicts suction feeding performance in centrarchid fishes. Journal of Experimental Biology 207:3873–3881.

Chen, L. C. 1985. A study of the *Sebastes inermis* species complex with delimitation of subgenus Mebarus (Pisces, Scorpaenidae). Journal of Taiwan Museum 38:23–37.

Chiba, S. 2004. Ecological and morphological patterns in communities of land snails of the genus *Mandarina* from the Bonin Islands. Journal of Evolutionary Biology 17:131–143.

Cody, M. L., and H. A. Mooney. 1978. Convergence versus nonconvergence in Mediterranean-climate ecosystems. Annual Review of Ecology and Systematics 9:265–321.

Drummond, A. J., M. A. Suchard, D. Xie, and A. Rambaut. 2012. Bayesian phylogenetics with BEAUti and the BEAST 1.7. Molecular Biology and Evolution 29:1969–1973.

Frédérich, B., L. Sorenson, F. Santini, G. J. Slater, and M. E. Alfaro. 2013. Iterative ecological radiation and convergence during the evolutionary history of damselfishes (Pomacentridae). American Naturalist 181:94–113.

Froese, R., and D. Pauly. 2013. FishBase. Accessed April 2013. www.fishbase.org.

Gillespie, R. G. 2004. Community assembly through adaptive radiation in Hawaiian spiders. Science 303:356–359.

Goatley, C. H. R., and D. R. Bellwood. 2009. Morphological structure in a reef fish assemblage. Coral Reefs 28:449–457.

Hansen, T. F. 1997. Stabilizing selection and the comparative analysis of adaptation. Evolution 51:1341–1351.

———. 2012. Adaptive landscapes and macroevolutionary dynamics. Pages 205–221 *in* E. I. Svennson and R. Calsbeek, eds. The adaptive landscape in evolutionary biology. Oxford University Press, Oxford.

Harmon, L. J., J. B. Losos, T. J. Davies, R. G. Gillespie, J. L. Gittleman, W. Bryan Jennings, K. H. Kozak, et al. 2010. Early bursts of body size and shape evolution are rare in comparative data. Evolution 64:2385–2396.

Harmon, L. J., J. T. Weir, C. D. Brock, R. E. Glor, and W. Challenger. 2008. GEIGER: investigating evolutionary radiations. Bioinformatics 24:129–131.

Hendry, C. R., T. J. Guiher, and R. A. Pyron. 2014. Ecological divergence and sexual selection drive sexual size dimorphism in new world pitvipers (Serpentes: Viperidae). Journal of Evolutionary Biology 27:760–771.

Hertz, P. E., Y. Arima, A. Harrison, R. B. Huey, J. B. Losos, and R. E. Glor. 2013. Asynchronous evolution of physiology and morphology in *Anolis* lizards. Evolution 677:2101–2113.

Huelsenbeck, J. P., R. Nielsen, and J. P. Bollback. 2003. Stochastic mapping of morphological characters. Systematic Biology 52:131–158.

Hyde, J. R., C. A. Kimbrell, J. E. Budrick, E. A. Lynn, and R. D. Vetter. 2008. Cryptic speciation in the vermilion rockfish (*Sebastes miniatus*) and the role of bathymetry in the speciation process. Molecular Ecology 17:1122–1136.

Hyde, J. R., and R. D. Vetter. 2007. The origin, evolution, and diversification of rockfishes of the genus *Sebastes* (Cuvier). Molecular Phylogenetics and Evolution 44:790–811.

Ingram, T. 2011. Speciation along a depth gradient in a marine adaptive radiation. Proceedings of the Royal Society B: Biological Sciences 278:613–618.

Ingram, T., and Y. Kai. 2014. Data from: The geography of morphological convergence in the radiations of Pacific *Sebastes* rock-

fishes. American Naturalist, Dryad Digital Repository, http://dx.doi.org/10.5061/dryad.s5s3s.

Ingram, T., and D. L. Mahler. 2013. SURFACE: detecting convergent evolution from comparative data by fitting Ornstein-Uhlenbeck models with stepwise Akaike Information Criterion. Methods in Ecology and Evolution 4:416–425.

Ingram, T., and J. B. Shurin. 2009. Trait-based assembly and phylogenetic structure in northeast Pacific rockfish assemblages. Ecology 90:2444–2453.

Jordan, D. S., and J. Z. Gilbert. 1920. Fossil fishes of diatom beds of Lompoc, California. Stanford University Publications, Stanford, CA.

Kai, Y., and T. Nakabo. 2008. Taxonomic review of the *Sebastes inermis* species complex (Scorpaeniformes: Scorpaenidae). Ichthyological Research 55:238–259.

———. 2013. Taxonomic review of the *Sebastes pachycephalus* complex (Scorpaeniformes: Scorpaenidae). Zootaxa 3637:546–560.

Kai, Y., K. Nakayama, and T. Nakabo. 2003. Molecular phylogenetic perspective on speciation in the genus *Sebastes* (Scorpaenidae) from the Northwest Pacific and the position of *Sebastes* within the subfamily Sebastinae. Ichthyological Research 50:239–244.

Kane, E. A., and T. E. Higham. 2012. Life in the flow lane: differences in pectoral fin morphology suggest transitions in station-holding demand across species of marine sculpin. Zoology 115:223–232.

Kendall, A. W., Jr. 2000. An historical review of *Sebastes* taxonomy and systematics. Marine Fisheries Review 62:1–23.

Kocher, T. D., J. A. Conroy, K. R. McKaye, and J. R. Stauffer. 1993. Similar morphologies of cichlid fish in Lakes Tanganyika and Malawi are due to convergence. Molecular Phylogenetics and Evolution 2:158–165.

Kozak, K. H., R. W. Mendyk, and J. J. Wiens. 2009. Can parallel diversification occur in sympatry? repeated patterns of body-size evolution in coexisting clades of North American salamanders. Evolution 63:1679–1784.

Lanfear, R., B. Calcott, S. Y. W. Ho, and S. Guindon. 2012. PartitionFinder: combined selection of partitioning schemes and substitution models for phylogenetic analyses. Molecular Biology and Evolution 29:1695–1701.

Lea, R. N., and J. E. Fitch. 1972. *Sebastes rufinanus*, a new scorpaenid fish from Californian waters. Copeia 1972:423–427.

Losos, J. B. 2010. Adaptive radiation, ecological opportunity, and evolutionary determinism. American Naturalist 175:623–639.

Losos, J. B., T. R. Jackman, A. Larson, K. Queiroz, and L. Rodriguez-Schettino. 1998. Contingency and determinism in replicated adaptive radiations of island lizards. Science 279:2115–2118.

Love, M. S., M. Yoklavich, and L. K. Thorsteinson. 2002. The rockfishes of the northeast Pacific. University of California Press, Berkeley, CA.

Mahler, D. L., and T. Ingram. 2014. Phylogenetic comparative methods for studying cladewide convergence. Pages 425–450 *in* L. Z. Garamszegi, ed. Modern phylogenetic comparative methods and their application in evolutionary biology: concepts and practice. Springer, New York.

Mahler, D. L., T. Ingram, L. J. Revell, and J. B. Losos. 2013. Exceptional convergence on the macroevolutionary landscape in island lizard radiations. Science 341:292–295.

Mahler, D. L., L. J. Revell, R. E. Glor, and J. B. Losos. 2010. Ecological opportunity and the rate of morphological evolution in the diversification of Greater Antillean anoles. Evolution 64:2731–2745.

Matsubara, K. 1943. Studies on the scorpaenoid fishes of Japan: anatomy, phylogeny and taxonomy. Vols. I, II. Sigenkagaku Kenkyusyo, Tokyo.

Muschick, M., A. Indermaur, and W. Salzburger. 2012. Convergent evolution within an adaptive radiation of cichlid fishes. Current Biology 22:2362–2368.

Muto, N., Y. Kai, and T. Nakabo. 2011. Genetic and morphological differences between *Sebastes vulpes* and *S. zonatus* (Teleostei: Scorpaeniformes: Scorpaenidae). Fishery Bulletin 109:429–439.

Muto, N., Y. Kai, T. Noda, and T. Nakabo. 2013. Extensive hybridization and associated geographic trends between two rockfishes *Sebastes vulpes* and *S. zonatus* (Teleostei: Scorpaeniformes: Sebastidae). Journal of Evolutionary Biology 26:1750–1762.

Nakabo, T., and Y. Kai. 2013. Sebastidae. Pages 565–595 *in* T. Nakabo, ed. Fishes of Japan with pictorial keys to the species. 3rd ed. Tokai University Press, Kanagawa, Japan.

Near, T. J., R. I. Eytan, A. Dornburg, K. L. Kuhn, J. A. Moore, M. P. Davis, P. C. Wainwright, M. Friedman, and W. L. Smith. 2012. Resolution of ray-finned fish phylogeny and timing of diversification. Proceedings of the National Academy of Sciences of the USA 109:13698–13703.

Neat, F. C., and N. Campbell. 2013. Proliferation of elongate fishes in the deep sea. Journal of Fish Biology 83:1576–1591.

Orr, J. W., and J. E. Blackburn. 2004. The dusky rockfishes (Teleostei: Scorpaeniformes) of the North Pacific Ocean: resurrection of *Sebastes variabilis* (Pallas, 1814) and a redescription of *Sebastes ciliatus* (Tilesius, 1813). Fishery Bulletin 102:328–348.

Orr, J. W., and S. Hawkins. 2008. Species of the rougheye rockfish complex: resurrection of *Sebastes melanostictus* (Matsubara, 1934) and a redescription of *Sebastes aleutianus* (Jordan and Evermann, 1898) (Teleostei: Scorpaeniformes). Fishery Bulletin 106:111–134.

Revell, L. J. 2009. Size-correction and principal components for interspecific comparative studies. Evolution 63:3258–3268.

———. 2012. phytools: an R package for phylogenetic comparative biology (and other things). Methods in Ecology and Evolution 3:217–223.

Ricklefs, R. E., and J. Travis. 1980. A morphological approach to the study of avian community organization. Auk 97:321–338.

Rutschmann, S., M. Matschiner, M. Damerau, M. Muschick, M. F. Lehmann, R. Hanel, and W. Salzburger. 2011. Parallel ecological diversification in Antarctic notothenioid fishes as evidence for adaptive radiation. Molecular Ecology 20:4707–4721.

Scheffer, M., and E. H. van Nes. 2006. Self-organized similarity, the evolutionary emergence of groups of similar species. Proceedings of the National Academy of Sciences of the USA 103:6230–6235.

Schluter, D. 1990. Species-for-species matching. American Naturalist 136:560–568.

———. 2000. The ecology of adaptive radiation. Oxford University Press, Oxford.

Simpson, G. G. 1953. The major features of evolution. Columbia University Press, New York.

Springer, M. S., M. J. Stanhope, O. Madsen, and W. W. de Jong. 2004. Molecules consolidate the placental mammal tree. Trends in Ecology and Evolution 19:430–438.

Stayton, C. T. 2008. Is convergence surprising? an examination of the frequency of convergence in simulated datasets. Journal of Theoretical Biology 252:1–14.

Stephens, P. R., and J. J. Wiens. 2009. Evolution of sexual size dimorphisms in emydid turtles: ecological dimorphism, Rensch's rule, and sympatric divergence. Evolution 63:910–925.

Thomas, G. H., and R. P. Freckleton. 2012. MOTMOT: models of

trait macroevolution on trees. Methods in Ecology and Evolution 3:145–151.

Valentin, A., J. M. Sévigny, and J. P. Chanut. 2002. Geometric morphometrics reveals body shape differences between sympatric redfish *Sebastes mentella*, *Sebastes fasdatus* and their hybrids in the Gulf of St. Lawrence. Journal of Fish Biology 60:857–875.

Venerus, L. A., J. E. Ciancio, C. Riva-Rossi, E. A. Gilbert-Horvath, A. E. Gosztonyi, and J. C. Garza. 2013. Genetic structure and different color morphotypes suggest the occurrence and bathymetric segregation of two incipient species of *Sebastes* off Argentina. Naturwissenschaften 100:645–658.

Wainwright, P. C., and B. A. Richard. 1995. Predicting patterns of prey use from morphology of fishes. Environmental Biology of Fishes 44:97–113.

Walker, J. A., and M. W. Westneat. 2002. Performance limits of labriform propulsion and correlates with fin shape and motion. Journal of Experimental Biology 205:177–187.

Warrant, E. J., and N. A. Locket. 2004. Vision in the deep sea. Biological Reviews 79:671–712.

Wiens, J. J. 2011. The niche, biogeography and species interactions. Philosophical Transactions of the Royal Society B: Biological Sciences 366:2336–2350.

Wright, D. I., W. J. O'Brien, and C. Luecke. 1983. A new estimate of zooplankton retention by gill rakers and its ecological significance. Transactions of the American Fisheries Society 112:638–646.

Associate Editor: David N. Reznick
Editor: Troy Day

A freckled rockfish (*Sebastes lentiginosus*). Photo credit: Travis Ingram and On Lee Lau.